

RSC Advances



This is an *Accepted Manuscript*, which has been through the Royal Society of Chemistry peer review process and has been accepted for publication.

Accepted Manuscripts are published online shortly after acceptance, before technical editing, formatting and proof reading. Using this free service, authors can make their results available to the community, in citable form, before we publish the edited article. This *Accepted Manuscript* will be replaced by the edited, formatted and paginated article as soon as this is available.

You can find more information about *Accepted Manuscripts* in the [Information for Authors](#).

Please note that technical editing may introduce minor changes to the text and/or graphics, which may alter content. The journal's standard [Terms & Conditions](#) and the [Ethical guidelines](#) still apply. In no event shall the Royal Society of Chemistry be held responsible for any errors or omissions in this *Accepted Manuscript* or any consequences arising from the use of any information it contains.



Journal Name

ARTICLE

An in-situ crosslinking approach towards chitosan-based semi-IPN hybrid particles for versatile adsorptions of toxins

Rui Wang^a, Xin Jiang^a, Ai He^a, Tao Xiang^{a*}, and Changsheng Zhao^{a,b**}Received 00th January 20xx,
Accepted 00th January 20xx

DOI: 10.1039/x0xx00000x

www.rsc.org/

The application of chitosan (CS) as adsorbent was limited by its poor acidic resistance, solubility in organic solvents and miscibility with synthetic polymers. In this study, an effective way was utilized to increase the amount of CS in hybrid particles together with good acid-alkali resistance and mechanical strength. CS was chemically modified and in situ cross-linked in polymer solutions to prepare hybrid particles with semi-interpenetrating network (semi-IPN) structure. Polyethersulfone (PES) was chosen as a representative polymer matrix to prepare hybrid particles; and the PES/CS-derivative particles exhibited good adsorption capacity to toxin bilirubin without procoagulant activity and adsorption capacity to Cu²⁺. Furthermore, the PES/CS-derivative hybrid particles exhibited selective adsorption to anionic dyes Congo red (CR) and environmental hormone bisphenol A (BPA) compared with other dyes or phenols. The results indicated the hybrid particles had versatile applications in blood purification and wastewater treatment.

Introduction

The removal of toxins that produced either in human body or environment was desired for human health. The internal toxins generally reach and harm some organs or tissues via blood circulation such as bilirubin,^{1,2} which could damage nervous system. On the other hand, the external toxins were usually from environmental pollutions, especially for water pollution in industrial field. Wastewater usually contains lots of toxins such as heavy metal ions, environmental hormones or organic dyes, which could destroy the growth environment of aquatic organism and enter into food chain to harm the human health.³ Thus, the removal of toxins is of great importance and there have been various methods such as filtration, adsorption, oxidation and degradation.⁴⁻⁶ Among these methods, adsorption is an effective method and has been extensively applied. Till now, various adsorbents have been reported such as clays,⁷ porous polymers,⁸ and carbon-based materials.⁹

Polymeric adsorbents could be easily processed into membranes^{10, 11} or particles,^{12, 13} and regenerated conveniently. More importantly, the specific functional groups such as COOH and NH₂ in some natural or synthetic polymers could give polymeric adsorbents selective adsorption ability.¹⁴⁻

¹⁶ Chitosan, a rare natural polymeric adsorbent which contains large amounts of amino groups, has been investigated as an adsorbent material.¹⁷⁻¹⁹ However, the poor solubility of chitosan in most solvents leads to poor processability and miscibility with other polymers, limiting its applications.²⁰ In addition, chitosan was susceptible to acidic solutions and its mechanical strength is usually not enough for using as long-term adsorbent. On the other hand, the reported methods to prepare chitosan-based composite materials could not increase the content of chitosan.²¹ Thus, the aim of this study is to provide a universal approach to prepare natural-synthetic hybrid adsorbents using chitosan derivatives and synthetic polymer matrixes to increase the amount of chitosan in the adsorbents.

In this paper, we synthesized some chitosan derivatives to increase its solubility in many common organic solvents, and studied its miscibility with synthetic polymers. PES has been widely used in the fields of biomedicine, food and water purification, due to its wide temperature limits, wide pH tolerances, and good chemical resistance to aliphatic hydrocarbons, alcohols, acids, etc.²² Thus, PES was chosen as a representative polymer matrix to prepare the hybrid particles by two methods, and the two methods were evaluated to choose an optimal way; then the acid-alkali resistance of the hybrid particles was investigated. As PES was widely used as blood-contacting materials especially in the area of hemodialysis, the removal of bilirubin for the hybrid particles was investigated. Cu²⁺ was chosen to investigate the heavy metal ion adsorption capability; Congo red (CR), rhodamine B (RhB) and methylene blue (MB) were used to study the dye adsorption capability; while bisphenol A (BPA), hydroquinone (HQ) and p-nitrophenol (HP) were chosen to study the phenol

^a College of Polymer Science and Engineering, State Key Laboratory of Polymer Materials Engineering, Sichuan University, Chengdu 610065, People's Republic of China.

^b National Engineering Research Center for Biomaterials, Sichuan University, Chengdu 610064, China.

† Electronic Supplementary Information (ESI) available: [data of adsorption kinetics and isotherms, images of acid-alkali resistance and mechanical property, XRD spectra of CS and CS derivatives, FTIR spectra of the particles, SEM images of PES/CS particles prepared by Method 1]. See DOI: 10.1039/x0xx00000x

adsorption capability. Furthermore, the adsorption kinetics and isotherms for BPA adsorption were also studied.

Materials and methods

Materials

Chitosan (CS, 98%, Aladdin), chlorotriphenylmethane (TrCl, 98%, Aladdin), diphenylmethane diisocyanate (MDI, 98%, Aladdin), bilirubin (98%, Aladdin), hydrazine monohydrate ($N_2H_4 \cdot H_2O$, 90%, Xiya reagent), polyethersulfone (PES, Ultrason E6020P, BASF) and phthalic anhydride (PA, 99%, Kelong) were used without further purification. Copper sulfate pentahydrate ($CuSO_4 \cdot 5H_2O$, 99%), bisphenol A (BPA, 98%), hydroquinone (HQ, 98%), p-nitrophenol (HP, 99%), Congo red (CR, 99%), rhodamine B (RhB, 99%) and methylene blue (MB, 99%) were obtained from Chengdu Kelong Chemical Reagent Co. Ltd. (China). N,N-dimethylacetamide (DMAc, 98%, Kelong), pyridine (98%, Kelong), N,N-dimethylformamide (DMF, 98%, Kelong), 1-methyl-2-pyrrolidinone (NMP, 98%, Kelong) and dimethyl sulfoxide (DMSO, 98%, Kelong) were distilled under vacuum. Deionized (DI) water was used throughout the study.

Synthesis of 2-Phthaloyl chitosan (PACS) and 2-Amino-6-O-triphenylmethyl chitosan (CSTr)

PACS was prepared according to the previous procedure.^{23, 24} Briefly, chitosan (4.00 g) was dispersed in a solution of phthalic anhydride (11.00 g) in DMF (150 mL), and the mixture was kept at 120 °C under nitrogen with vigorous stirring for 8 h. After the reaction, the solution was cooled to room temperature and poured into water. The precipitate was washed with water and ethanol, and then dried under vacuum at 40 °C to give 7.50 g of the product (PACS).

To synthesize CSTr, the amino groups should be protected firstly due to their higher reactivity than hydroxyl groups.^{25, 26} Firstly, chlorotriphenylmethane (47.9 g) was added into a solution of PACS (5.00 g) in pyridine (75 mL) and the reaction was carried out at 90 °C for 24 h. After removing most of the solvent by using a rotary evaporator, the residue was washed with ethanol and dried under vacuum at 40 °C to obtain 2-phthaloyl-6-O-triphenylmethyl chitosan (PACSTr). Then, PACSTr (4.00 g) was dispersed in a mixture of hydrazine monohydrate (20 mL) and water (40 mL), and the solution was heated with stirring under nitrogen at 100 °C for 24 h. After being cooled, the mixture was diluted with water and rotated evaporation. The residue was washed with ethanol and ether, and dried under vacuum at 25 °C to give 2.60 g of the product (CSTr).

The FTIR spectra were recorded with KBr pellets on a Nicolet-560 spectrophotometer (USA).

¹H NMR (400 MHz) spectra were recorded on a Bruker AVII-400MHz spectrometer (Bruker Co., Germany), using tetramethylsilane (TMS) as the internal standard in DMSO-*d*₆.

Preparation of PES/CS hybrid particles, PES/CSTr and SI-PES/CSTr hybrid particles

As shown in Scheme 1, PES/CS hybrid particles were prepared by a two-step method termed as Method 1. The mixed solution of PACS and PES was prepared into particles by

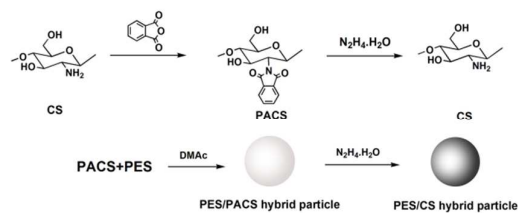
a liquid-liquid phase separation technique as described in our earlier report.²⁷ In order to get regular and smooth particles, the solution was dropped into sodium dodecyl sulfate (SDS) (0.05 wt.%) aqueous solution. The total concentration of PACS and PES was controlled at 12 wt.%, and the mass ratios of PACS were controlled at 0%, 25%, 50%, respectively. After washing with DI water, the prepared hybrid particles were applied into a mixture of hydrazine monohydrate (20 mL) and water (40 mL), and incubated at 80 °C with stirring for 24 h to remove the phthaloyl groups. The final hybrid particles were washed with DI water for several times and termed as PES/CS-25 and PES/CS-50, respectively.

The method to prepare the hybrid particles with semi-IPN structure (SI-PES/CSTr) is termed as Method 2 and also shown in Scheme 1. The total concentration of PES and CSTr was 12 wt.%, and the mass ratios of the CSTr were controlled at 25% and 50%. Then MDI solution in little DMAc were dropwise added into the mixed solutions with stirring to crosslink CSTr in situ at room temperature for 0.5 h, and the content of MDI was controlled at 2 wt.% of the CSTr. The liquid-liquid phase separation technique as described in Method 1 was used to prepare the hybrid particles and the hybrid particles were termed as SI-PES/CSTr-25 and SI-PES/CSTr-50, respectively. Additionally, PES/CSTr hybrid particles without crosslinking were also prepared as comparisons and were termed as PES/CSTr-25 and PES/CSTr-50, respectively. The final hybrid particles were placed into DI water for 24 h to remove the residual DMAc.

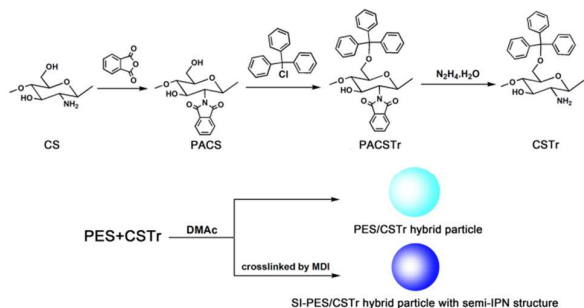
The morphologies of prepared particles were characterized by scanning electron microscopy (SEM, JSM-7500F, JEOL).

The actual weight ratios of CS or CS derivatives in the hybrid particles was calculate by TGA (TG 209 FI, NETZSCH), which scanned at a temperature ranging from 30 to 800 °C, and at a heating rate of 10 °C /min under nitrogenous gas.

Method 1



Method 2



Scheme 1. The schematic illustration for preparing PES/CS, PES/CSTr and SI-PES/CSTr particles using Method 1 and Method 2, respectively.

Acidic-alkali resistance of the particles

To measure the acidic and alkali resistances, 20 hybrid particles (about 0.018 g in dry weight) were immersed in 10 mL of 0.01 M HCl solution, 2 wt.% acetic acid solution (HOAc) or 0.01 M NaOH solution at room temperature for 24 h with oscillation, respectively. Subsequently, the hybrid particles were washed with DI water and then dried in a vacuum oven at 40 °C, then, the contents of CS or CS derivatives were measured by TGA.

Adsorption to bilirubin

Blood compatibility of materials is an important standard for the removal of bilirubin from blood to ensure the materials have no procoagulant activity. Thus, activated partial thromboplastin time (APTT) and thrombin time (TT) were measured firstly as described in the previous studies.²⁸

To prepare bilirubin solution, bilirubin were firstly dissolved in little 0.1 M NaOH solution and then diluted with PBS (pH=7.4) to control the concentration at 0.15 mg/mL. Then 40 particles (about 0.036 g in dry weight) were applied in 10 mL bilirubin solution with oscillation at 25 °C. The concentrations were determined by an UV-vis spectrometer (UV-1750, Shimadzu) at the wavelength of 438 nm.

Adsorption to environmental toxins

To investigate Cu²⁺ adsorption, 40 particles (about 0.036 g) were immersed in 10 mL of 10 mmol/L CuSO₄ aqueous solution at 25 °C with oscillation. The concentration of Cu²⁺ was measured by an atomic adsorption spectroscopy (SPCA-626D, Shimadzu).

Congo red (CR), rhodamine B (RhB) and methylene blue (MB) were chosen as representatives of anionic and cationic dyes. The initial concentrations of the dye aqueous solutions were controlled at 200 μmol/mL and 20 particles (about 0.018 g) were applied in 10 mL of the respective aqueous solutions which were carried out at 25 °C with oscillation. The concentrations were determined at different time intervals by an UV-vis spectrometer at the wavelength of 497, 554 and 630 nm, respectively.

To study the adsorption ability to different phenols, bisphenol A (BPA), hydroquinone (HQ) and p-Nitrophenol (NP) were chosen as the adsorbates. 20 particles (about 0.018 g) were applied in 10 mL of the respective aqueous solutions at 25 °C with oscillation. The concentrations were determined at different time intervals by an UV-vis spectrometer at the wavelength of 276, 288 and 317 nm, respectively.

The desorption experiments for Cu²⁺, CR and BPA were carried out as follows: after the adsorption reached equilibrium, for the Cu²⁺ desorption, 40 hybrid particles (about 0.036 g) with maximum adsorption were immersed into 10 mL of EDTA aqueous solution (0.01 mol/L) or hydrochloric acid (pH 2), respectively; while for the CR and BPA desorption, 20 hybrid particles (about 0.018 g) were applied into 10 mL of hydrochloric acid (pH 2) or ethanol, respectively. After 24 h, the concentrations of the desorbed adsorbate in the EDTA solution, hydrochloric acid solution or ethanol solution were determined by atomic adsorption spectroscopy or UV-vis spectrometer, respectively, and the solutions were replaced by

fresh ones for the next desorption process. This process was carried for three turns. In each turn, the desorption ratio (R_d) was obtained as:

$$R_d = \frac{n_d}{n_a} \times 100\% \quad (1)$$

where n_d is the desorbed amount in each time; n_a is the total adsorbed amount by the particles, which is calculated from the adsorption experiment. The total desorption ratios are the sum of the R_d for the three turns.

Results and discussion

Characterization of the chitosan derivatives

The FTIR spectra of CS, PACS and CSTr are shown in Figure 1 (a). Compared with the spectrum of CS, the spectrum of PACS showed new peaks at 1715 and 1287 cm⁻¹, which were attributed to the C=O bonds from the imide groups and the ester bonds from low amount of the *O*-phthaloyl groups, respectively. The spectrum of CSTr showed new peaks at 1659, 1597 and 1491 cm⁻¹, which were assigned to the benzene ring from triphenylmethane groups; while the peak at 1715 cm⁻¹ from the phthaloyl groups disappeared, which indicated that the phthaloyl groups were dissociated successfully.

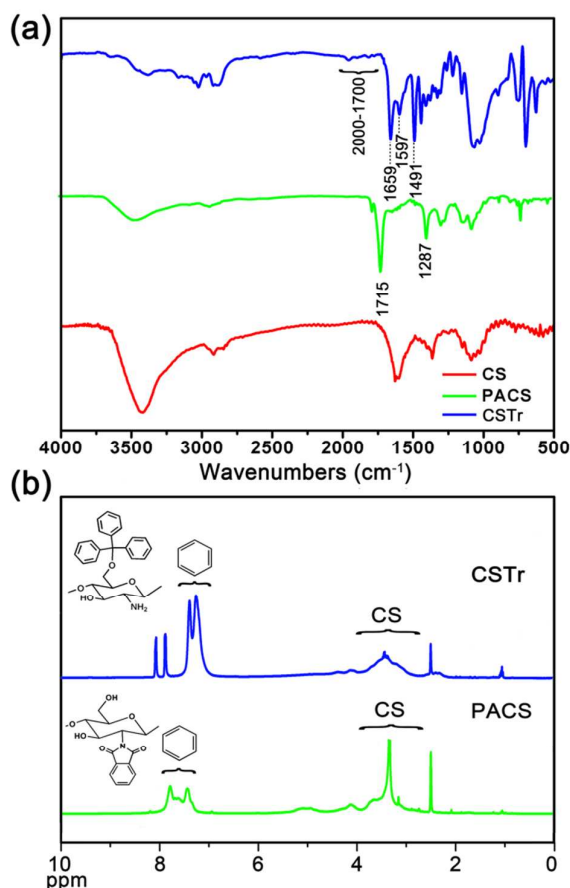


Figure 1. (a) FTIR spectra of CS, PACS and CSTr; (b) ¹H NMR spectra of PACS and CSTr.

The ^1H NMR ($\text{DMSO-}d_6$) spectra of PACS and CSTR are shown in Figure 1 (b). The peaks at 2.0 to 4.5 ppm were assigned to the hydrogens of chitosan. The peaks at 7.78 and 7.43 ppm in the spectrum of PACS were attributed to the hydrogens of the benzene ring from the phthaloyl groups; while the peaks at 7.39 and 7.26 ppm in the CSTR spectrum were assigned to the hydrogens of the benzene ring from the triphenylmethane groups. The results indicated that the phthaloyl groups or triphenylmethane groups were grafted into CS chains successfully.

The N-substitution or O-substitution also affected the crystallinity of the CS derivatives. The images of X-ray diffraction diagrams (XRD, see Figure S1) showed that the pristine CS had crystallinity; while the PACS was amorphous due to the N-substitution and partial O-substitution,²³ and CSTR had partial crystallinity. Thus, the solubility of PACS and CSTR in organic solvents could be improved compared with CS (see Table S1), which provided the possibility for blending with other polymer matrixes.

Acid-alkali and solvent resistances of the particles

TGA was performed to calculate the actual weight ratios of CS or its derivatives in the hybrid particles and the results are shown in Figure 2 (a). Method 1 is a more convenient method due to the fewer steps than Method 2. However, the CS contents in the PES/CS-25 and PES/CS-50 particles prepared by Method 1 decreased sharply, indicating that most of CS was washed out in removing phthaloyl groups. The contents of CSTR in the SI-PES/CSTR-25 and SI-PES/CSTR-50 particles prepared by Method 2 were 24 wt.% and 46 wt.%, respectively, which were similar to the designed contents, indicating that Method 2 was a more effective approach to prepare the hybrid particles. On the other hand, for the PES/CSTR, the decomposition peak temperature of CSTR was 249°C , while that for the SI-PES/CSTR slightly increased to 254°C , demonstrating the existence of semi-IPN structure. It could be also observed that the CSTR contents in SI-PES/CSTR particles were slightly higher than that in PES/CSTR and the results indicated that the in-situ crosslinking approach could maintain more CSTR. Thus, the following studies were based on the SI-PES/CSTR and PES/CSTR particles prepared by Method 2.

Acid and alkali resistances were important properties for adsorption materials. Pristine CS has poor acidic or alkali resistance and could be dissolved in 0.01 M HCl or 2 wt.% HOAc aqueous solution, and degraded in alkaline solution.^{29,30} However, the modification of CS could change the hydrophilicity and polarity of CS, while the in-situ crosslinking could immobilize the CSTR in the particles to provide more stable structure, thus the acid-alkali resistance was improved significantly. As shown in Figure 2 (b), the CSTR contents only slightly decreased for either PES/CSTR or SI-PES/CSTR hybrid particles under the acid and alkali conditions, exhibiting good acid-alkali resistance. Furthermore, the weight loss for the SI-PES/CSTR particles with semi-IPN structure was lower than that for the PES/CSTR particles, demonstrating better acid-alkali resistances provided by the in-situ crosslinking approach.

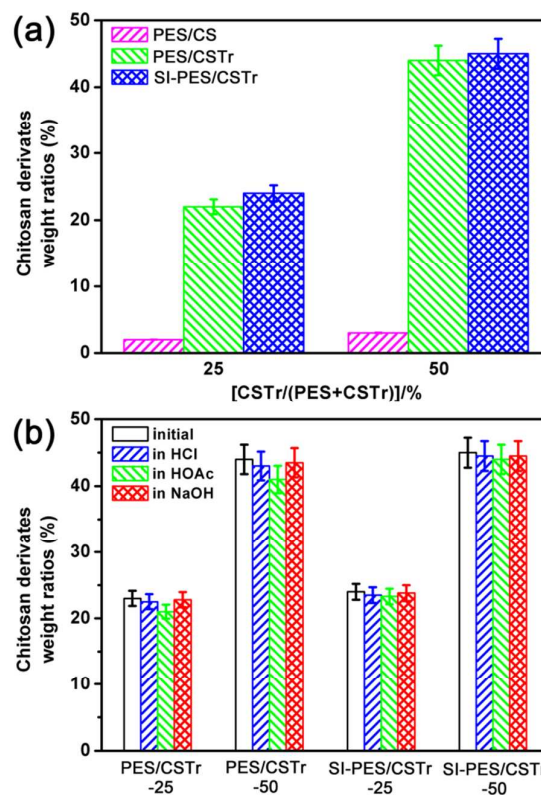


Figure 2. (a) The contents of CS or CSTR in hybrid particles measured by TGA; (b) The contents of CSTR in PES/CSTR and SI-PES/CSTR particles measured by TGA after immersing in HCl, HOAc and NaOH solutions, respectively.

Further studies indicated that the SI-PES/CSTR had better solvent resistance than PES/CSTR against DMAC (see Figure S2). In addition, the mechanical property enhanced obviously (see Figure S3) compared with the pristine CS particles.

Morphology of the particles

SEM was performed to investigate the morphologies of the particles. As shown in Figure 3, the pristine PES particle was regular sphere, and the finger-like structure was observed clearly.³¹ With the increase of CSTR content both for PES/CSTR and SI-PES/CSTR particles, the shape of the particles became oblate spheroid and the finger-like structure reduced. For the PES/CSTR-25 and SI-PES/CSTR-25 particles with the same designed CSTR content, the morphology of the skin layer was similar to the pristine PES particle, while the internal structure changed and the porous structure became compact. However, for PES/CSTR-50 and SI-PES/CSTR-50, though the designed CSTR content was the same, the morphologies of two particles were significantly different. For the PES/CSTR-50 particle, the pore structure and finger-like structure disappeared completely, and many microspheres appeared in the whole particle, which may be caused by the phase separation with high CSTR content;^{32, 33} while for the SI-PES/CSTR-50 particle, the microspheres were fewer and the pore structure in the skin layer could be observed. The results indicated that the semi-

IPN structure formed by in-situ crosslinking could immobilize the CSTR and reduce the phase separation during the particle preparation.

The morphologies of surfaces for the pristine PES, PES/CSTR-50 and SI-PES/CSTR-50 were also observed as shown in Figure 4. The PES had smooth surface and no pores appeared in the surface; while large pores appeared in the surface of PES/CSTR-50, which might be caused by the phase separation and loss of CSTR. However, for the SI-PES/CSTR-50, fewer pores with smaller size appeared in the surface. The results further demonstrated that the in situ crosslinking could provide more stable structure which could affect either internal structure or surface structure.

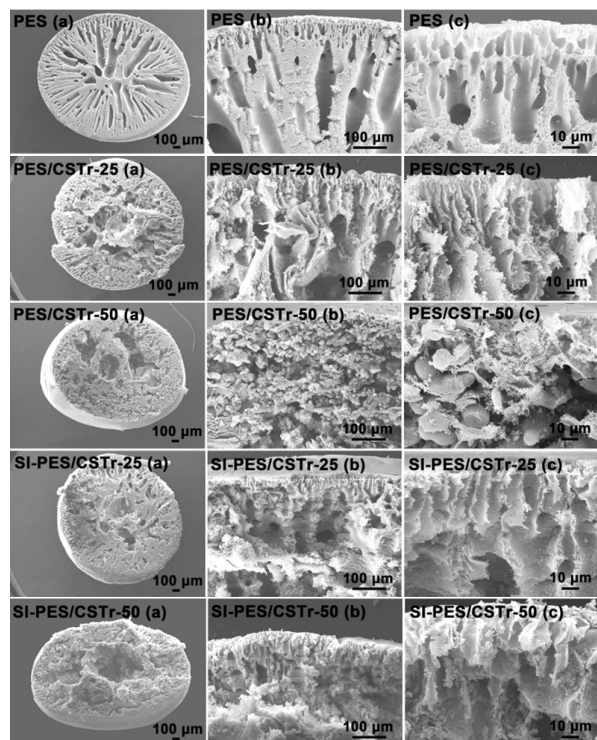


Figure 3. SEM pictures of cross-sections for PES, PES/CSTR-25, PES/CSTR-50, SI-PES/CSTR-25 and SI-PES/CSTR-50 particles.

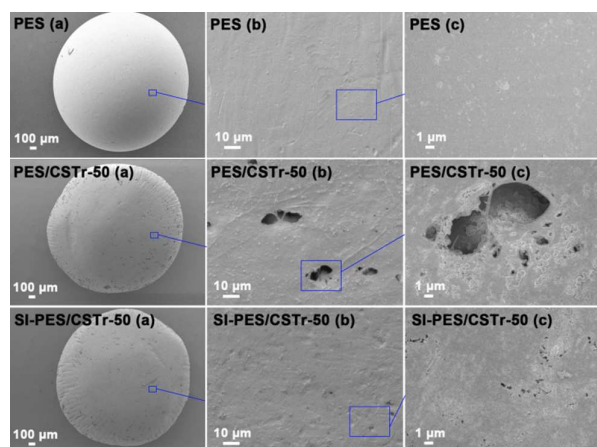


Figure 4. SEM pictures of surfaces for PES, PES/CSTR-50, and SI-PES/CSTR-50 particles.

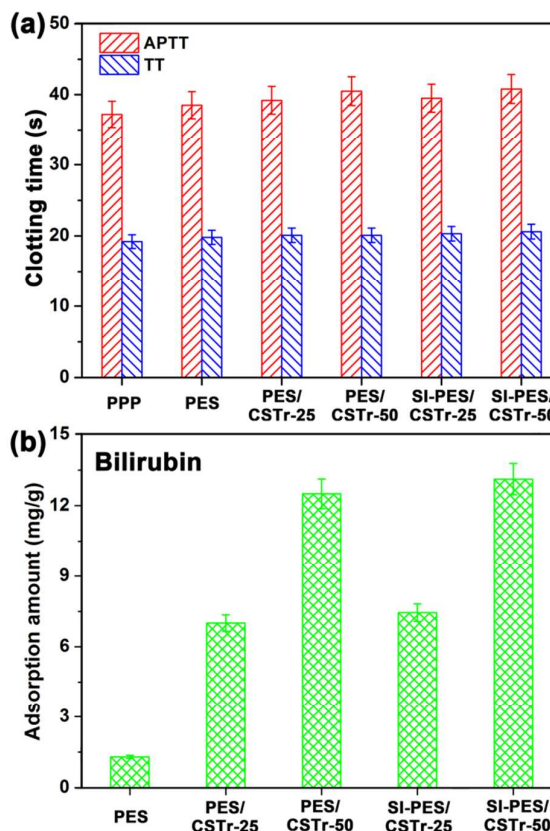


Figure 5. (a) APTT and TT values of the PPP, pristine PES and hybrid particles; (b) The bilirubin adsorbed amounts per unit for pristine PES and hybrid particles after 2 h.

Bilirubin adsorption

Blood-contacting materials usually require materials have good blood compatibility and no procoagulant activity firstly. APTT is a performance indicator of the efficacy of the intrinsic and common plasma coagulation pathway; while TT was used to measure the clot formation time taken for the thrombin conversion of fibrinogen into fibrin.³⁴ As shown in Figure 5 (a), the clotting time of the hybrid particles were not reduced compared with the platelet-poor plasma (PPP) and pristine PES. Since PES has been widely used as blood-contacting materials, the results demonstrated that the hybrid particles had no procoagulant activity and may have potential used as blood-contacting materials.

The adsorption amount of bilirubin after 2 h was shown in Figure 5 (b). Pristine PES particles have low adsorption content of bilirubin; while with the increase of CSTR content, the adsorption amount for SI-PES/CSTR-50 increased remarkably reaching a maximum of 13.12 mg/g. The results indicated that the CSTR could endow PES with adsorption capacity to bilirubin, and the hybrid particles had potential application as blood purification material. Additionally, it could be observed that the adsorption amount for SI-PES/CSTR was higher than that of PES/CSTR, demonstrating that the hybrid particles with semi-IPN structure had more effective CSTR content used for adsorbing, which could also reflected by the results of IECs

(see Figure S4). As the in-situ crosslinking could limit the weight loss of the CSTR and formation of microspheres, this approach could provide more effective CSTR content to increase the adsorption amount.

Cu²⁺ Adsorption

Cu²⁺ was chosen as the representative to investigate the adsorption to heavy ion and the adsorbed amounts per unit mass of the particles are shown in Figure 6. The adsorption amount increased with the increase of CSTR mass ratios which could reach a maximum of 15.12 mg/g, and the adsorption reached equilibrium after about 50 h (see Figure S8). In addition, the adsorption amounts for SI-PES/CSTR-25 and SI-PES/CSTR-50 were higher than those for the respective PES/CSTR-25 and PES/CSTR-50, similar with the results of IECs and bilirubin adsorption. The result demonstrated once again that the semi-IPN structure could enhance the adsorption capacity, and the hybrid particles might have potential application to remove heavy ions from wastewater.

Adsorptions to CR, RhB and MB

CR and RhB are anionic dyes with potential carcinogenicity,³⁵ while MB is cationic dye. The CR, RhB and MB adsorbed amounts per unit mass of PES and SI-PES/CSTR-50 particles at pH 7 are shown in Figure 7 (a). Owing to the large amount of amino groups, the molecules bearing negative charges could be adsorbed. Thus, the CR and RhB adsorbed amounts for the SI-PES/CSTR-50 particles were significantly higher than that of the pristine PES particles, especially for CR adsorption; while the MB adsorbed amount for SI-PES/CSTR was the lowest among the three dyes and close to that of PES, which indicated that the hybrid particles have selective adsorption capability to anionic dyes in according with other chitosan-based adsorbents as previous reports.^{35, 36} Figure 7 (b) showed that the CR adsorbed amount increased with the increase of the CSTR mass ratios. The adsorbed amounts for the PES, PES/CSTR-25, PES/CSTR-50, SI-PES/CSTR-25 and SI-PES/CSTR-50 particles were 29.45, 50.36, 64.06, 57.31 and 69.47 mg/g, respectively. All the adsorption processes could reach equilibrium after about 50 h (see Figure S9).

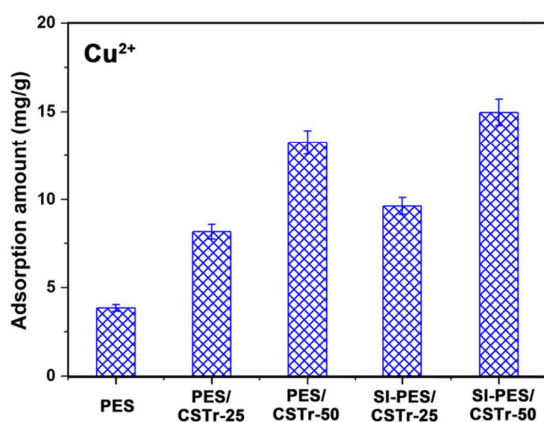


Figure 6. Cu²⁺ adsorbed amounts per unit mass for pristine PES and hybrid particles.

To further investigate the adsorption capacity of hybrid particles that were based on different synthetic polymer matrixes, polyvinylidene fluoride (PVDF) and polysulfone (PSF) were used to prepare the SI-PVDF/CSTR-50 and SI-PSF/CSTR-50 particles, and the results of CR adsorption are shown in Figure 7 (c). As shown in figure, the CR adsorbed amounts for the modified particles were higher obviously than those for the pristine synthetic polymer particles, which demonstrated that CSTR could be used to prepare hybrid particles with different synthetic polymers. In addition, the adsorption amount of SI-PES/CSTR-50 was the highest among other modified particles with PVDF or PSF, indicating that PES was the optimized polymer matrix to prepare CS-based absorbent.

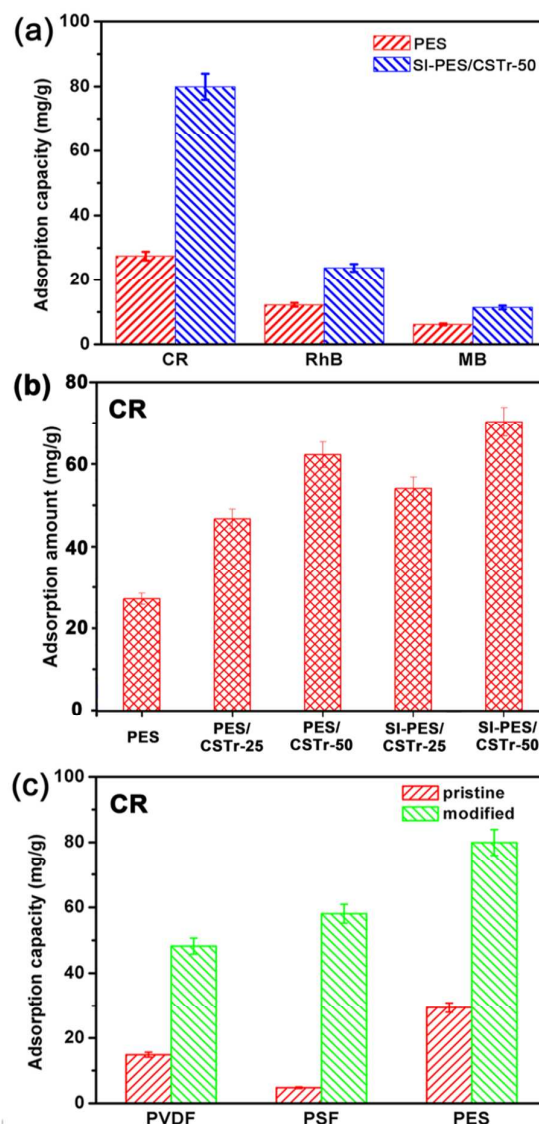


Figure 7. (a) The CR, RhB and MB adsorptions for PES and SI-PES/CSTR-50 particles. (b) The CR adsorbed amounts per unit mass for pristine PES and hybrid particles. (c) The CR adsorbed amounts per unit mass for PES, PVDF, PSF, SI-PES/CSTR-50, SI-PVDF/CSTR-50 and SI-PSF/CSTR-50 particles, respectively.

Compared with the previous reports, the SI-PES/CSTr particles could reach similar adsorption amount at the same concentration.^{35, 36} Together with the good morphologies, mechanical property and acid-base resistance of the hybrid particles compared with some chitosan-based adsorbents, the SI-PES/CSTr particles had potential application as the adsorbents to remove CR in wastewater treatment.

Adsorptions to BPA, HQ, and NP

BPA, HQ, and NP are three types of phenols and BPA is an environmental hormone which could interfere with the endocrine system. The BPA, HQ, and NP equilibrated adsorbed amounts at pH 7 for the PES, PES/CSTr-50 and SI-PES/CSTr-50 particles are shown in Figure 8 (a). The BPA adsorbed amounts for the PES/CSTr-50 and SI-PES/CSTr-50 particles were obviously higher than that for the pristine PES, while the HQ and NP adsorbed amounts were closed to these for PES particles. The results indicated that the hybrid particles had selective adsorption character for BPA at pH 7, which would have potential application to selectively remove BPA from wastewater. This result might be caused by the existence of hydrophobic groups in BPA and CSTr, which could reduce the molecule polarity and hydrophilicity. Thus, the binding capability increased due to the similar polarity and chemical groups. On the other hand, despite that PES is more hydrophobic than CSTr, the PES had polar groups such as sulphone groups, which could increase the physical adsorption capacity to polar molecules such as NP. Thus, owing to the existences of the sulphone groups in PES, the NP adsorption for the PES was higher than that for the SI-PES/CSTr-50.

The effect of concentration on the BPA adsorption amount was also investigated and the results are given in Figure 8 (b). As shown in the figure, the adsorbed amounts increased with the increase of the concentration, which could be attributed to the increased contacting probability between the BPA molecules and the adsorbing sites in the particles. In addition, the concentration could accelerate the diffusion of the BPA molecules into the hybrid particles.⁹

The BPA adsorbed amount increased with the increase of the CSTr mass ratios in the particles as shown in Figure 8 (c), and the adsorbed BPA amounts for the PES, PES/CSTr-25, PES/CSTr-50, SI-PES/CSTr-25 and SI-PES/CSTr-50 were 7.23, 11.96, 15.38, 12.00 and 16.58 mg/g, respectively. It could be observed that the BPA adsorbed amounts to the SI-PES/CSTr particles were higher than those to the PES/CSTr particles, which was similar to the results of adsorptions to bilirubin, Cu²⁺ and CR, and further indicated that the semi-IPN structure had a positive effect on the adsorptions to different toxins.

On the other hand, previous studies investigated the NP or BPA adsorption amount at different concentrations.^{37, 38} Compared with the previous studies, at the same concentration of NP used in this study (200 μmol/L, 27.8 mg/L), the adsorption amount for the hybrid particles was higher (about 12 mg/g) than that in the previous study (about 5 mg/g). For BPA adsorption, the SI-PES/CSTr-50 could reached the similar adsorption amount at lower concentration (200 μmol/L, 45.6 mg/L) compared with the previous study (100-200 mg/L).

These results indicated that the SI-PES/CSTr particles may have more effective adsorption capacity at lower concentration of NP or BPA, and this might be beneficial to apply in wastewater treatment.

Furthermore, three kinetic models (pseudo-first-order, pseudo-second-order and intraparticle diffusion) were used to analyse the BPA adsorption in this study. The pseudo-first-order kinetic model is more suitable for low concentration of solute.³⁹ It can be represented in the following form:⁴⁰

$$\ln(q_e - q_t) = \ln q_e - k_1 t \quad (2)$$

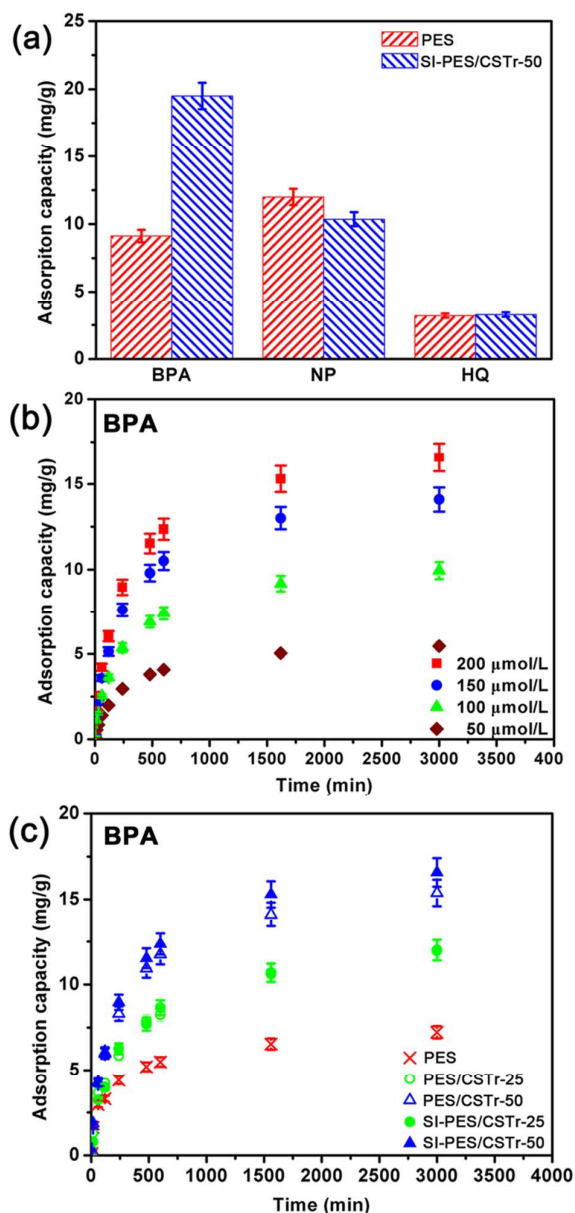


Figure 8. (a) The BPA, NP and HQ adsorptions to the pristine PES and SI-PES/CSTr-50 particles. (b) The BPA adsorbed amounts per unit mass for the SI-PES/CSTr-50 particles with various initial concentrations. (c) The BPA adsorbed amounts per unit mass for the pristine PES and hybrid particles.

where q_t is the BPA amount adsorbed at time t (mg/g); q_e is that adsorbed at the equilibrium (mg/g); k_1 is the rate constant of pseudo-first-order equation.

the pseudo-second-order is dependent on the amount of the solute adsorbed on the surface of adsorbent and the amount adsorbed at equilibrium, and the equation was expressed in the following form:⁴⁰

$$\frac{t}{q_t} = \frac{1}{k_2 q_e^2} + \frac{t}{q_e} \quad (3)$$

where k_2 is the rate constant of pseudo-second-order equation; q_t , q_e , and t have the same meaning as those in the pseudo-first-order equation.

Besides, the intraparticle diffusion model could identify the diffusion mechanism and the equation can be written in the following form:⁴¹

$$q_t = k_p t^{1/2} + C \quad (4)$$

where k_p is the rate constant of intraparticle diffusion model, C is a constant for any experiment (mg/g), q_t has the same meaning as that in Eq. (3).

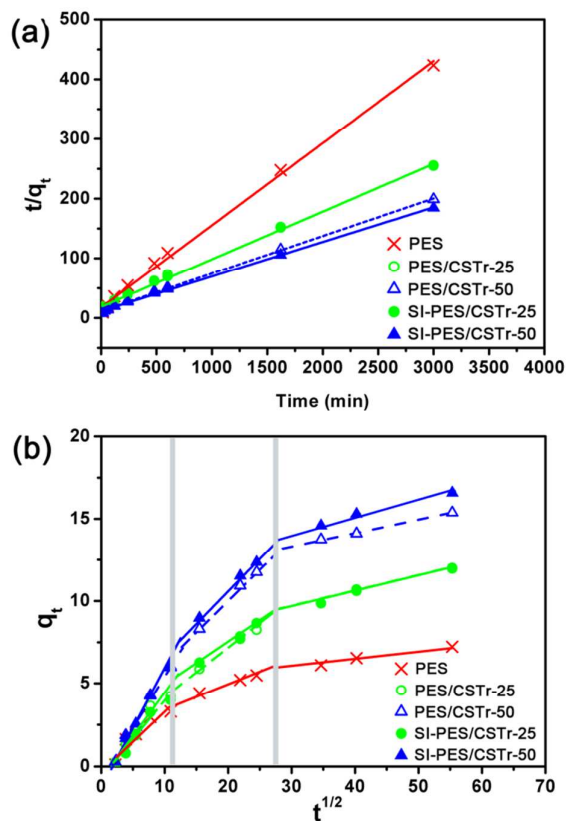


Figure 9. (a) Application of the pseudo-second-order adsorption model for the BPA adsorption onto the pristine PES and hybrid particles. (b) The intraparticle diffusion model for the BPA adsorption onto the pristine PES and hybrid particles.

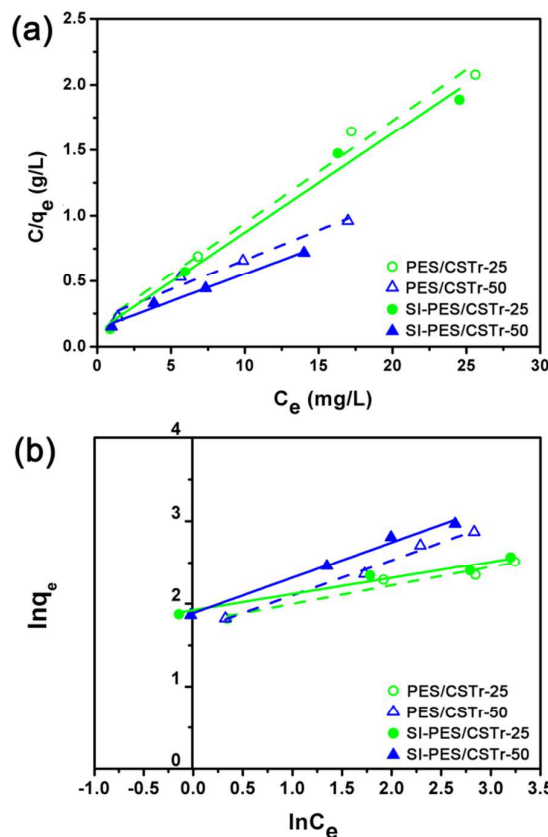


Figure 10. (a) Application of Langmuir adsorption isotherm of PES/CSTr and SI-PES/CSTr particles. (b) Application of Freundlich adsorption isotherm of PES/CSTr and SI-PES/CSTr particles.

The results of BPA adsorption indicated that the data did not agree well with the pseudo-first-order kinetic model, but prefer fitted the pseudo second-order and intraparticle diffusion model as shown in Figure 9. For the pseudo second-order model, the rate constant (k_2) and the equilibrium adsorption capacity (q_e) could be obtained and all the correlation coefficients (r_2) were higher than 0.99 (see in Table S2), indicating that the adsorption to PBA fitted the pseudo second-order model well. For the intraparticle diffusion model, the three slopes in each curve indicated that there were three diffusion steps during the adsorption process: the first step was the external surface adsorption or diffusion in macropores. The second step was the gradual adsorption step and was controlled by intraparticle diffusion. The third step was the final equilibrium step, for which the adsorbent molecules moved slowly from larger pores to micro-pores and caused a slow adsorption rate. The rate constant (k) for three steps can be obtained and all the correlation coefficients (r_2) were higher than 0.98 (see in Table S3).

The adsorption isotherms were also analysed including Langmuir and Freundlich adsorption isotherm. The Langmuir adsorption isotherm has been successfully applied to many adsorption processes and the equation is as follows:

$$\frac{C_e}{q_e} = \frac{1}{q_{\max} k_L} + \frac{C_e}{q_{\max}} \quad (5)$$

where q_e is the mass of the BPA adsorbed by the unit mass after the adsorption reaches equilibrium (mg/g); C_e is the equilibrium concentration of the BPA (mg/L); q_{\max} is the maximal adsorbed amount of the particles (mg/g); k_L is the Langmuir adsorption constant. As shown in Figure. 10 (a), a plot of C_e/q_e versus C_e give a straight line with the slope of $1/q_{\max}$ and the intercept $C_e/(q_{\max})$. All the correlation coefficient (r_2) were higher than 0.98 (see Table S4), which indicated that the adsorption to PBA on the PES/CSTr and SI-PES/CSTr particles followed the Langmuir adsorption isotherm.

The Freundlich isotherm⁴² is an empirical equation, and its form is as follows:

$$q_e = k_F C_e^{1/n} \quad (6)$$

where k_F is the Freundlich isotherm constant; q_e and C_e has the same meaning as that in Eq. (5); $1/n$ is the influence coefficient of solution concentration to the equilibrium adsorbed amount. The linear form of the Freundlich isotherm equation can be obtained by the following equation:

$$\ln q_e = k_F + (1/n) \ln C_e \quad (7)$$

A linear plot was obtained when $\ln q_e$ was plotted against $\ln C_e$, as shown in Figure. 10 (b), and then the parameters could be obtained (see Table S4). The values of the correlation coefficient were higher than 0.95, and some of them could reach 0.99. It indicated that the adsorption process also fitted this model. The above results suggested that both of the monolayer Langmuir adsorption isotherm and Freundlich isotherm were suitable for explaining the adsorption process.

Desorption of Cu^{2+} , CR and PBA from the hybrid particles

The Cu^{2+} desorption experiments were carried out in EDTA aqueous solution (0.01 M) and hydrochloric acid aqueous solution (pH 2) using the SI-PES/CSTr-50 particles. The desorbed ratios for three repeating times are given in Figure 11 (a). As shown in the figure, the desorbed ratios for each time in EDTA and HCl were similar, and the total desorbed ratios were higher than 0.95. With the good acid-base resistance, it suggested that the SI-PES/CSTr-50 particles after Cu^{2+} adsorption could be regenerated easily using EDTA or HCl solution.

The CR and BPA desorption experiments were carried out in ethanol solution and hydrochloric acid aqueous solution (pH 2), and the results are shown in Figure 11 (b) and Figure 11 (c). As shown in the figures, the first desorbed ratios in EtOH were higher than that in HCl for both CR and BPA, since EtOH is the good solvent for CR and BPA. The total desorbed ratios could be over 0.95 in both EtOH and HCl solution, which indicated that the hybrid particles after BPA or CR adsorption could be regenerated easily using EtOH or HCl. Together with the good acid-base resistance and mechanical properties, the SI-PES/CSTr particles may have wide practicability in the wastewater treatment and could be utilized circularly.

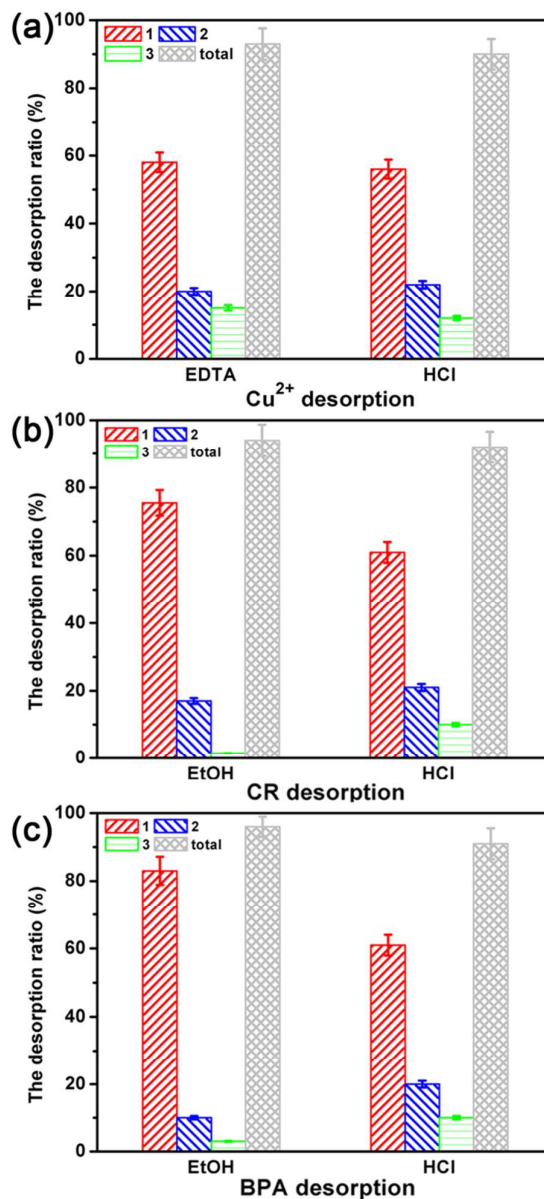


Figure 11. (a) The desorption ratios of Cu^{2+} in EDTA and HCl aqueous solution, respectively. (b) The desorption ratios of CR in HCl aqueous solution and ethanol, respectively. (c) The desorption ratios of BPA in HCl aqueous solution and ethanol, respectively.

Conclusion

In this work, chitosan-based hybrid particles were prepared by two methods using synthetic polymer matrices. The in-situ crosslinking approach using 2-amino-6-*O*-triphethylmethyl chitosan was proved to be an effective way to increase the content of chitosan, and could be used to prepare hybrid particles with synthetic polymers such as PVDF, PSF and PES. PES was chosen as the reprehensive polymer matrix to prepare hybrid particles with semi-IPN structure. The hybrid particles with semi-IPN structure exhibited better acid-alkali

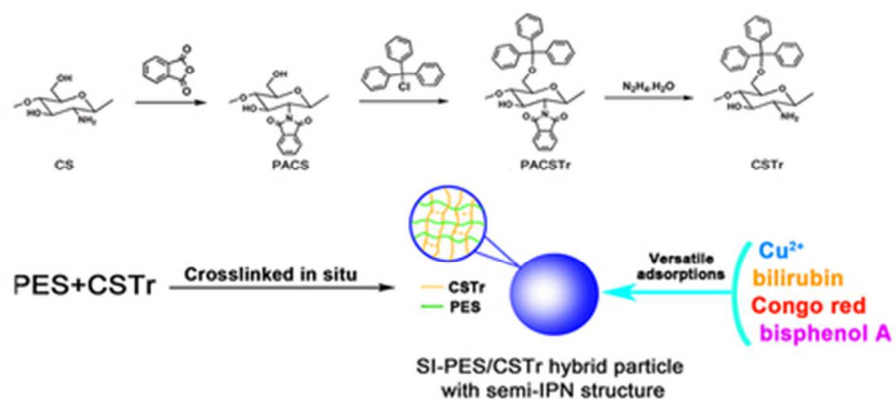
resistance and mechanical property compared with the pristine chitosan particles, and exhibited good adsorption capacity to toxin bilirubin without procoagulant activity. In addition, the hybrid showed good adsorption capacity to Cu²⁺ and selective adsorption capability to anionic dyes CR and RhB at neutral pH condition. Furthermore, the hybrid particles had selective adsorption to BPA among BPA, NP and HQ, and the BPA adsorption process agreed well to the pseudo-second-order model and intraparticle diffusion model, and fitted with Langmuir isotherm and Freundlich isotherm. We anticipated that this approach to prepare chitosan-based hybrid particles with semi-IPN structure could provide a route to improve the versatile adsorption capability and make some potential contributions to the fields of blood purification and wastewater treatment.

Acknowledgement

This work was financially sponsored by the National Natural Science Foundation of China (No. 51225303 and 51433007), and the Programme of Introducing Talents of Discipline to Universities (B13040). We should also thank our laboratory members for their generous help, and gratefully acknowledge the help of Ms. Hui. Wang, of the Analytical and Testing Center at Sichuan University, for the SEM.

References

1. K. Yamazaki, K. Shinke and T. Ogino, *Colloid Surface B*, 2013, **112**, 103-107.
2. T. Asano, K. Tsuru, S. Hayakawa and A. Osaka, *Acta Biomaterialia*, 2008, **4**, 1067-1072.
3. Y. F. Lin, H. W. Chen, P. S. Chien, C. S. Chiou and C. C. Liu, *J Hazard Mater*, 2011, **185**, 1124-1130.
4. R. P. S. Suri, J. C. Crittenden and D. W. Hand, *J Environ Eng-Asce*, 1999, **125**, 897-905.
5. K. Rzeszutek and A. Chow, *Talanta*, 1998, **46**, 507-519.
6. Z. F. Guo, R. X. Ma and G. J. Li, *Chemical Engineering Journal*, 2006, **119**, 55-59.
7. J. M. Pan, X. H. Zou, X. Wang, W. Guan, C. X. Li, Y. S. Yan and X. Y. Wu, *Chemical Engineering Journal*, 2011, **166**, 40-48.
8. B. O. Yoon, S. Koyanagi, T. Asano, M. Hara and A. Higuchi, *Journal of Membrane Science*, 2003, **213**, 137-144.
9. A. He, B. Lei, C. Cheng, S. Li, L. Ma, S. D. Sun and C. S. Zhao, *Rsc Adv*, 2013, **3**, 22120-22129.
10. J. J. Wu, H. W. Lee, J. H. You, Y. C. Kau and S. J. Liu, *J Colloid Interf Sci*, 2014, **420**, 145-151.
11. K. K. R. Tetala and D. F. Stamatialis, *Sep Purif Technol*, 2013, **104**, 214-220.
12. Y. Jiang and D. Kim, *Chemical Engineering Journal*, 2013, **232**, 503-509.
13. X. L. Zhu, X. L. Gu, L. N. Zhang and X. Z. Kong, *Nanoscale Res Lett*, 2012, **7**.
14. Q. W. Tang, X. M. Sun, Q. H. Li, J. M. Lin and J. H. Wu, *J Mater Sci*, 2009, **44**, 726-733.
15. J. X. Han, Z. J. Du, W. Zou, H. Q. Li and C. Zhang, *J Hazard Mater*, 2014, **276**, 225-231.
16. X. T. Sun, L. R. Yang, Q. Li, J. M. Zhao, X. P. Li, X. Q. Wang and H. Z. Liu, *Chemical Engineering Journal*, 2014, **241**, 175-183.
17. M. L. G. Vieira, V. M. Esquerdo, L. R. Nobre, G. L. Dotto and L. A. A. Pinto, *J Ind Eng Chem*, 2014, **20**, 3387-3393.
18. X. H. Wang, L. Yang, J. P. Zhang, C. Y. Wang and Q. Y. Li, *Chemical Engineering Journal*, 2014, **251**, 404-412.
19. P. Liu and Z. X. Su, *Mater Lett*, 2006, **60**, 1137-1139.
20. S.-K. Kim, *Chitin and chitosan derivatives: Advances in drug discovery and developments*, CRC Press, 2013.
21. X. F. Zeng and E. Ruckenstein, *Journal of Membrane Science*, 1996, **117**, 271-278.
22. C. S. Zhao, J. M. Xue, F. Ran and S. D. Sun, *Prog Mater Sci*, 2013, **58**, 76-150.
23. K. Kurita, H. Ikeda, Y. Yoshida, M. Shimojoh and M. Harata, *Biomacromolecules*, 2002, **3**, 1-4.
24. K. Kurita, H. Ikeda, M. Shimojoh and J. Yang, *Polym J*, 2007, **39**, 945-952.
25. S. I. Nishimura, O. Kohgo, K. Kurita and H. Kuzuhara, *Macromolecules*, 1991, **24**, 4745-4748.
26. W. Sajomsang, *Carbohydr Polym*, 2010, **80**, 631-647.
27. C. S. Zhao, Q. R. Wei, K. G. Yang, X. D. Liu, M. Nomizu and N. Nishi, *Sep Purif Technol*, 2004, **40**, 297-302.
28. Y. Xia, C. Cheng, R. Wang, H. Qin, Y. Zhang, L. Ma, H. Tan, Z. W. Gu and C. S. Zhao, *Polym Chem-Uk*, 2014, **5**, 5906-5919.
29. M. N. V. R. Kumar, *React Funct Polym*, 2000, **46**, 1-27.
30. A. Bhatnagar and M. Sillanpaa, *Adv Colloid Interfac*, 2009, **152**, 26-38.
31. W. Zou, Y. Huang, J. Luo, J. Liu and C. S. Zhao, *Journal of Membrane Science*, 2010, **358**, 76-84.
32. F. Ran, S. Q. Nie, W. F. Zhao, J. Li, B. H. Su, S. D. Sun and C. S. Zhao, *Acta Biomater*, 2011, **7**, 3370-3381.
33. M. Kuang, H. W. Duan, J. Wang and M. Jiang, *J Phys Chem B*, 2004, **108**, 16023-16029.
34. S. Q. Nie, M. Tang, C. Cheng, Z. H. Yin, L. R. Wang, S. D. Sun and C. S. Zhao, *Biomater Sci-Uk*, 2014, **2**, 98-109.
35. S. Chatterjee, S. Chatterjee, B. P. Chatterjee and A. K. Guha, *Colloid Surface A*, 2007, **299**, 146-152.
36. T. Feng, S. Xiong and F. Zhang, *Desalin Water Treat*, 2015, **53**, 1970-1976.
37. J. M. Li, X. G. Meng, C. W. Hu and J. Du, *Bioresource Technol*, 2009, **100**, 1168-1173.
38. J. M. Pan, H. Yao, X. X. Li, B. Wang, P. W. Huo, W. Z. Xu, H. X. Ou and Y. S. Yan, *J Hazard Mater*, 2011, **190**, 276-284.
39. M. Doğan, Y. Özdemir and M. Alkan, *Dyes Pigment.*, 2007, **75**, 701-713.
40. S. S. Gupta and K. G. Bhattacharyya, *J Hazard Mater*, 2006, **128**, 247-257.
41. X. Y. Yang and B. Al-Duri, *J. Colloid Interface Sci.*, 2005, **287**, 25-34.
42. F. M. Cao, P. L. Bai, H. C. Li, Y. L. Ma, X. P. Deng and C. S. Zhao, *J. Hazard. Mater.*, 2009, **162**, 791-798.



The schematic illustration for preparing PES/CS, PES/CSTr and SI-PES/CSTr particles using Method 1 and Method 2, respectively.
39x19mm (300 x 300 DPI)